Received December 2004
Revised August 2005
Accepted September 2005

Flow around a circular cylinder in an external magnetic field at high Reynolds numbers

T.V.S. Sekhar
Department of Mathematics, Pondicherry Engineering College, Pondicherry, India
R. Sivakumar
Department of Physics, Pondicherry Engineering College, Pondicherry, India, and
T.V.R. Ravi Kumar
Department of Applied Mathematics, Ideal College of Arts and Sciences, Kakinada, India

Abstract

Purpose – To study the steady viscous incompressible electrically conducting fluid flow past a circular cylinder under the influence of an external magnetic field at high Reynolds numbers (*Re*).

Design/methodology/approach – The finite difference method is applied to solve the governing non-linear Navier-Stokes equations. First order upwind difference scheme is applied to the convective terms. The multigrid method with coarse grid correction is used to enhance the convergence rate. The defect correction technique is employed to achieve the second order accuracy.

Findings – A non-monotonic behavior in separation angle when $N \geq 5$ and separation length when $N \geq 3$ is found with the increase of external magnetic field. The drag coefficient is found to increase with increase of N. The pressure drag coefficient, total drag coefficient and rear pressure are found to exhibit a linear dependence with $N^{0.5}$. The pressure Poisson equation is solved to find pressure fields in the flow region. It is found that the upstream base pressure increases with increase of external magnetic field while the downstream base pressure decreases with the increase of the external magnetic field.

Originality/value – The non-monotonic behaviors in the separation angle and separation length at high *Re* are explained through pressure fields which are found first time for this problem. The linear dependence of the pressure drag coefficient, total drag coefficient and the pressure at rear stagnation point with $N^{0.5}$ is in agreement with experimental findings.

Keywords Flow, Fluids, Finite difference methods

Paper type Research paper

1. Introduction

The structure of steady viscous incompressible flow over a circular cylinder at high Reynolds number (*Re*) forms one of the classical problems in fluid mechanics.

The authors are thankful to Prof. Umamaheswara Rao, Department of Applied Mathematics. Andhra University, Visakhapatnam for his encouragement. The authors are also grateful to Dr Raghurama Rao, Department of Aerodynamics, Indian Institute of Science, Bangalore for useful discussion.

International Journal of Numerical Methods for Heat & Fluid Flow
Vol. 16 No. 6, 2006
pp. 740-759

0961-5539
DOI 10.1108/09615530610679084

Some notable studies on this problem in the 1970s are given by Dennis and Chang (1970), Takami and Keller (1969) and Robert Leigh Underwood (1969). They provided solutions up to $Re = 10$, 60 and 100, respectively. In Fornberg (1980) provided numerical solutions for the steady viscous flow past a circular cylinder at *Re*s up to 300 using Newton's method. In Fornberg (1985) he further extended his approach to high *Re*s up to 600. He found that the wake bubble (region with recirculating flow) grows in length approximately linearly with *Re*. The width increases like $\sqrt{Re}$ up to $Re = 300$ at which point a transition to linear increase with *Re* begins. At very high *Re*s the wake resembles a pair of translating, uniform vortices, both touching the center line. Later, Fornberg (1988) studied the steady viscous flow past a sphere for the high *Re*s $100 \leq Re \leq 5{,}000$ using the Newton's method. The steady flow past a rotating circular cylinder is studied by Tang and Ingham (1991) at *Re*s 60 and 100. The computation of high *Re* flow around a circular cylinder with surface roughness is studied by Kawamura and Kuwahara (1984). The physical analysis of the pressure and velocity fields in the near wake of a circular cylinder is investigated by Braza *et al.* (1986). Williamson studied oblique and parallel modes of vortex shedding in the wake of a circular cylinder at low *Re*s (Welliamson, 1989). It has been shown experimentally (Norberg, 2003; Williamson, 1996a) and theoretically (Thompson and Le Gal, 2004) that the flow about a circular cylinder becomes unstable at around $Re = 47$ where Hopf bifurcation occurs leading to periodic shedding of vortices from the upper and lower side of the cylinder. Jackson (1987) showed that the first instability leading to the von Karman vortex street arises at $Re \sim 49$. The nature of the secondary instability towards a spanwise-periodic 3D flow at $Re \sim 188$ is also investigated (Henderson and Barkely, 1996; Williamson, 1996b). Lima E Silva *et al.* (2003) simulated this problem using the immersed boundary method.

1.1 Effect of magnetic field on the flow

It is well known that the effect of a suitable magnetic field on an electrically conducting fluid controls the growth of a boundary layer which is an undesirable flow feature in many engineering cases. The boundary layer separation causes increase of drag and diminished pressure recovery which are hurdles to many practical applications, especially with regard to transport in fluids. Therefore, a lot of attention is given by researchers to control the flow separation. Recent experimental works in this area can be found in Weir *et al.* (1998, 2000, 2001, 2003). Greenblatt and Wyganski (2000) studied the control of flow separation using periodic excitation. Bae *et al.* (2001) investigated the suppression of Karmann vortex excitation of a circular cylinder by a second cylinder set downstream in a cruciform arrangement. Recently, Baranyi (2003) studied the unsteady momentum and heat transfer from a fixed cylinder in an aligned magnetic field. Raghava Rao and Sekhar (1993, 1995) found the suppression of separation in the rotating flow past a sphere. They found vortex jump phenomena at higher *Re*s and Taylor numbers. Experimentally Lahjomri *et al.* (1993) established that two-dimensional instability (vortex shedding) can be suppressed. There is a view in magnetohydrodynamics that constant (steady) magnetic field can damp any instabilities, something that is found in metallurgical or crystal growth applications. For the flow past a cylinder in an aligned magnetic field (Mutschke *et al.*, 1998) has shown that the magnetic field influences 2D and 3D instabilities in a different way and three-dimensional steady flow does exist (Mutschke *et al.*, 1997).

Later Mutschke *et al.* (2001) further discussed the scenario of three-dimensional instabilities in the magnetohydrodynamic cylinder flow when the oncoming flow and the magnetic field are parallel. They found a non monotonic behavior of the 3D instability when the strength of the magnetic field is increased. All known experimental results about 2D stability are restricted to relatively high *Re* because of serious measuring problems in liquid mental flows. Maxworthy (1968) achieved pressure distribution measurements around a sphere placed in a sodium flow aligned with the magnetic field at infinity. For an interaction parameter ranging from 0 to 40 he concluded that the upstream pressure initially rises continuously as N increases and reaches an asymptotic value when $N > 15$, placing a limit on the upstream zone contribution to the sphere pressure drag. Meanwhile, the downstream base pressure as N increase due to the loss in total pressure head a fluid particle undergoes, when crossing the magnetic field. The association of these two phenomena is consequently responsible for an increase with N of the pressure drag coefficient which was found proportional to $\sqrt{N}$ when $N > 5$. A similar behavior has also been reported by Yonas (1967), who made direct drag measurements on spheres and disks in a sodium flow for interaction parameter values up to 80. The fact that the asymptotic dependence with N of the drag coefficient seems to be independent of the shape of the body is probably one of the most important results of Maxworthy's and Yonas' study. Josserand *et al.* (1993) in their experimental work on a cylinder in a liquid metal flow, studied the angular evolution of the pressure around a cylinder in an MHD flow aligned with the magnetic field for value of the interaction parameter between 0 and 8. Recently using numerical simulation Sekhar *et al.* (2005) investigated the steady incompressible flow around a sphere in an aligned magnetic field and the result concur with the findings of Maxworthy, Yonas and Josserand *et al.* In this paper we consider the incompressible flow around a circular cylinder with a magnetic field aligned with the flow at infinity for the range of *Re* between 100 and 500 and with an interaction parameter up to 12. The vorticity-stream function formulation of the Navier-Stokes equations is used and solved with finite difference method. The multigrid method with defect correction technique is employed to achieve the second order accurate solution.

2. Formulation of the problem

The governing equations for the steady state, viscous and incompressible magnetohydrodyamic axisymmetric flow is solved in the cylindrical coordinate system. The free stream velocity is $\mathbf{U}_\infty$ is from left to right and the applied magnetic field $\mathbf{H}$ is parallel to this flow. The viscosity, conductivity, density and permeability of the fluid are η, σ, ρ, and μ, respectively, and the radius of the cylinder is a. The curl of the momentum equation and the equation of continuity in the non-dimensional form are:

$$\nabla^2\omega = \frac{Re}{2}[\nabla \times (\omega \times q)] - \frac{NRe}{2}[\nabla \times \{(q \times \mathbf{H}) \times \mathbf{H}\}] \tag{1}$$

in which:

$$\omega = \nabla \times q \tag{2}$$

$$\nabla \cdot q = 0 \tag{3}$$

where q is the fluid velocity and ω is the vorticity. The Re is given by $Re = 2\rho U_\infty a/\eta$ and $N = \sigma H_\infty^2 a/\rho U_\infty$ is the interaction parameter. The following non-dimensional terms are substituted to obtain the dimensionless differential equations:

$$q = \frac{\mathbf{q}'}{U_\infty}, \quad p = \frac{a}{\rho \nu U_\infty} p', \quad r = \frac{r'}{a}, \quad \mathbf{H} = \frac{\mathbf{H}'}{H_\infty}$$

$$\mathbf{E} = \frac{\mathbf{E}'}{E_\infty}, \quad \mathbf{j} = \frac{\mathbf{j}'}{j_\infty}$$

where primed variables are dimensional quantities and v is the kinematic viscosity, E_∞ and j_∞ are the magnitudes of electric field intensity and current density at infinity, respectively. The dimensionless stream function $\psi(r,\theta)$ is introduced so that the equation of continuity (equation (3)) is satisfied:

$$q_r = \frac{1}{r}\frac{\partial \psi}{\partial \theta}, \quad q_\theta = -\frac{\partial \psi}{\partial r} \tag{4}$$

where q_r and q_θ are the dimensionless radial and transverse components of fluid velocity.

The polar coordinates (r,θ) are used in such a way that the flow is symmetric about $\theta = 0°$ and $\theta = 180°$. As the magnetic field and fluid flow are aligned at infinity, the electric field can be assumed to be zero. The problem is simplified by assuming the magnetic Re to be small ($R_m \ll 1$, where, R_m is defined as the ratio of the induced magnetic field to the imposed magnetic field) so that the magnetic field can be taken as a constant, given by:

$$\mathbf{H} = (-\cos\theta, \sin\theta, 0) \tag{5}$$

This simplification will eliminate nonlinear terms of unknown quantities in the Maxwell's equations. Substitution of equation (4) in equations (2) and (4), equation (5) in equation (1) with the transformation $r = e^{\pi\xi}$ and $\theta = \pi\eta$ yields, in the vorticity-stream function form as follows:

$$\frac{\partial^2 \psi}{\partial \xi^2} + \frac{\partial^2 \psi}{\partial \eta^2} + \pi^2 e^{2\pi\xi}\omega = 0 \tag{6}$$

$$\begin{aligned} &\frac{\partial^2 \omega}{\partial \xi^2} + \frac{\partial^2 \omega}{\partial \eta^2} - \frac{Re}{2}\left[\frac{\partial \psi}{\partial \eta}\frac{\partial \omega}{\partial \xi} - \frac{\partial \psi}{\partial \xi}\frac{\partial \omega}{\partial \eta}\right] \\ &\quad = \frac{NRe}{2}\left[\pi^2 e^{2\pi\xi}\omega \sin^2(\pi\eta) + \sin 2(\pi\eta)\frac{\partial^2 \psi}{\partial \xi \partial \eta}\right. \\ &\quad\quad \left. - \pi \sin 2(\pi\eta)\frac{\partial \psi}{\partial \eta} - \cos 2(\pi\eta)\frac{\partial^2 \psi}{\partial \xi^2} + \pi \cos 2(\pi\eta)\frac{\partial \psi}{\partial \xi}\right] \end{aligned} \tag{7}$$

Equations (6) and (7) must now be solved subject to the following boundary conditions.

On the surface of the cylinder $(\xi = 0) : \psi = \partial\psi/\partial\xi = 0, \quad \omega = -(1/\pi^2)(\partial^2\psi/\partial\xi^2)$

At large distances from the cylinder $(\xi \to \infty) : \psi \sim e^{\pi\xi}\sin(\pi\eta), \quad \omega \to 0$

Along the axis of symmetry $(\eta = 0 \text{ and } \eta = 1) : \psi = 0, \quad \omega = 0$

The following pressure Poisson equation, which is obtained by taking the divergence of the Navier-Stokes equations, is then solved to find the pressure in the flow field.

$$-(p_{\xi\xi} + p_{\eta\eta}) = \frac{2}{r^2\pi^2}\left[(\psi_{\xi\eta} - \pi\psi_\eta)^2 - (\psi_{\xi\xi} - \pi\psi_\xi)(\psi_{\eta\eta} + \pi\psi_\xi)\right] +$$

$$\frac{N}{r^2\pi^2}\left[\frac{\sin(2\pi\eta)}{2}(\psi_{\xi\xi} - \psi_{\eta\eta} - 2\pi\psi_\xi) + \cos(2\pi\eta)(\psi_{\xi\eta} - \pi\psi_\eta)\right]$$

with boundary conditions

On the surface of the cylinder $(\xi = 0) : p_\xi = -(2/Re)\omega_\eta$

At large distances from the cylinder $(\xi \to \infty) : p = 1$

Along the axis of symmetry $(\eta = 0 \text{ and } \eta = 1) : p_\eta = 0.$

3. Numerical method

The coupled nonlinear Navier-Stokes equations are solved by applying finite difference method and the resulting algebraic equations are solved by using the multigrid method.

Here, a recursive multigrid procedure is employed in which the smoother is a point Gauss Seidel iteration and the usual coarse grid correction is applied (Juncu, 1999).

The initial solution is taken as $\psi = 0$ and $\omega = 0$ at all inner grid points except for ψ at $\xi = \infty$ where the boundary condition holds. In finding the solution for higher values of *Re* and *N*, the solution obtained for lower values of *Re* and *N* are used as starting solution. Convergence is said to have been achieved when the difference between two successive iterations m and $m + 1$, at all interior grid points, is less than 10^{-7}, i.e.:

$$|\psi^{m+1} - \psi^m| < 10^{-7} \quad \text{and} \quad |\omega^{m+1} - \omega^m| < 10^{-7}.$$

We used the injection operator as restriction operator throughout this study. For the prolongation operator the simplest from is derived using linear interpolation. The 9-point prolongation operator defined by Wesseling (1980) is used for the present study.

The solution obtained by the above method is not second order accurate as we have approximated all terms by second order central differences except convective terms which are approximated by first order upwind difference scheme to ensure diagonal dominance. In order to achieve second order accurate solution, the defect correction method is employed as follows. For example, if B is the operator obtained by first order upwind discretization and A is that obtained by second order accurate discretization, then defect correction algorithm (Juncu, 1999) works as given below. At the start of defect correction, $\bar{y}$ is a solution that is not second order accurate, and at the end of defect correction, $\bar{y}$ is second order accurate.

begin Solve $B\bar{y} = b$
  for $i := 1$ step 1 until n do
    solve $By = b - A\bar{y} + B\bar{y}$
    $\bar{y} := y$
  od
end

Usually, in practice, it is sufficient to take $n = 1$ or 2.

4. Results and discussions

The second order accurate results are obtained from the finest grid 512 × 512 when $N < 1$ and 1,024 × 1,024 when $N \geq 1$. The effect of magnetic field on the streamlines for $Re = 100$, 300 and 500 are shown in Figures 1-3, respectively. It is evident from these figures that the applied magnetic field delays (suppresses) the separation at rear stagnation point, and that suppression of the recirculation bubble is not complete. A non-monotonic behavior in recirculation length is found when $N \geq 3$ and in separation angle when $N \geq 5$ for all Re considered in this study as shown in Figure 4. For $Re = 100$ the recirculation length decrease up to $N = 2$ and then slowly increases up to $N = 12$. For $Re = 300$ and 500 the recirculation length decreases up to $N = 2$ and then increases up to $N = 6$ and again decreases with increase of magnetic field. The boundary layer separation angle initially decreases until $N = 5$ and then increases

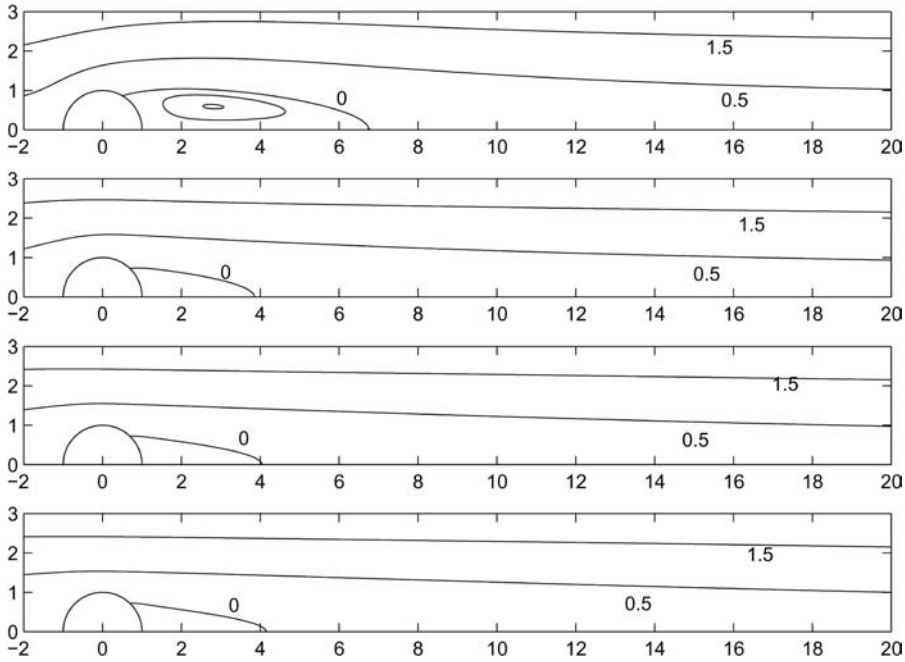

Figure 1.
Streamlines for $Re = 100$, $N = 0.2$, 2, 6 and 12 (top to bottom)

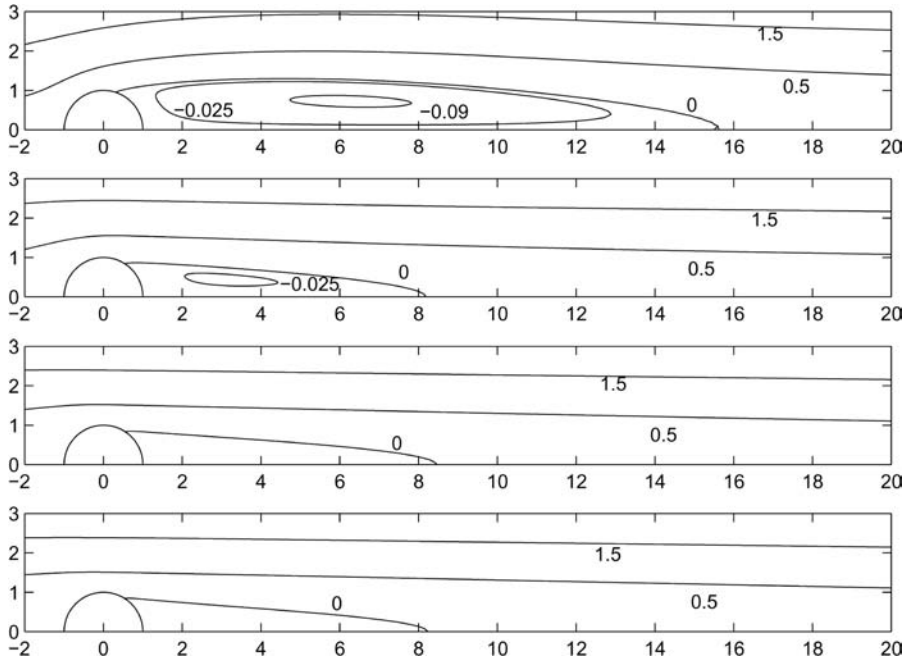

Figure 2.
Streamlines for $Re = 300$, $N = 0.2$, 2, 6 and 12 (top to bottom)

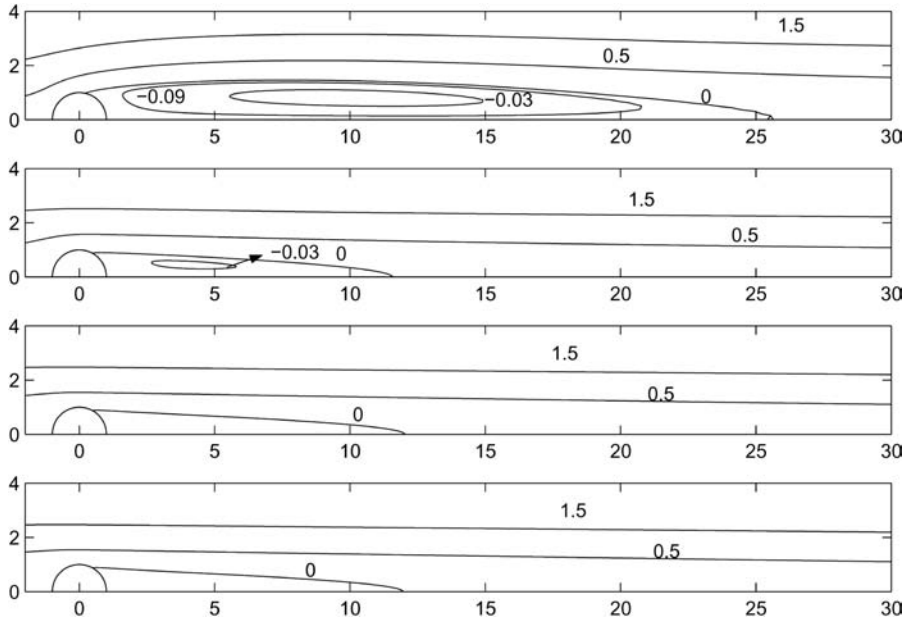

Figure 3.
Streamlines for $Re = 500$, $N = 0.2$, 2, 6 and 12 (top to bottom)

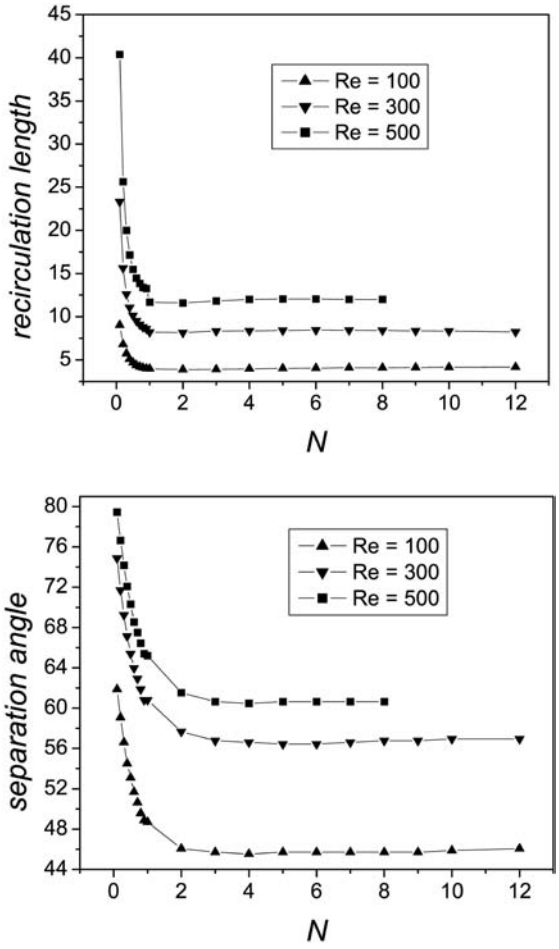

Figure 4.
Dependance of recirculation length l and separation angle θ on interaction parameter N

when $N > 5$. It is observed that as magnetic field increases (higher values of N), the flow becomes straightened in the main stream direction and the curvature of the recirculation bubble (i.e. $\psi = 0$) decreases. The flow inside the recirculation bubble slows down monotonically with increasing magnetic field. As the magnetic forces are proportional to and resist the flow of fluid in any other direction than that of the unperturbed magnetic field near the cylinder, they produce changes in the pattern of the vorticity lines. The length of the standing vortex is reduced and the strength of the disturbance upstream and downstream of the cylinder is increased with increasing magnetic field. Also, a growing inviscid rotational region is found at higher values of N which is predicted theoretically (Banks and Zaturska, 1984; Leibovich, 1967). These features can be seen from the figures of iso-vorticity contours as shown in Figure 5 for $Re = 500$. It is clear from Figure 6 that the magnetic field tends to suppress the surface vorticity behind the cylinder.

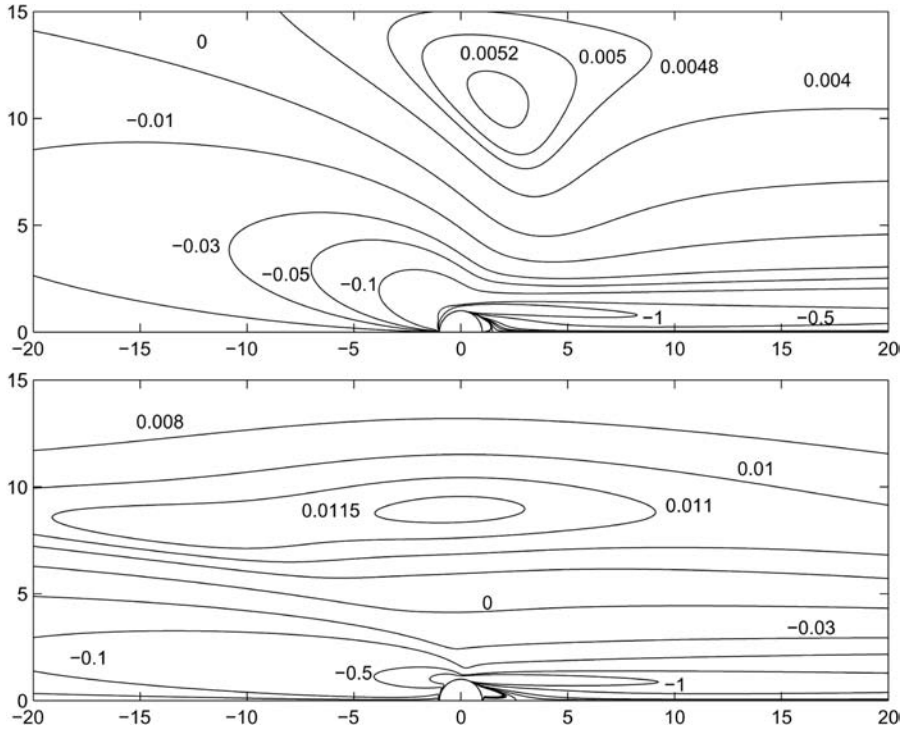

Figure 5.
Isocontours of vorticity for $Re = 500$, $N = 1$ (top) and $N = 8$ (bottom)

It is found that the upstream base pressure increases continuously with increase of N, while downstream base pressure decreases with increase of N. The angular evolution of the surface pressure is shown in Figure 7. The pressure at rear stagnation point is found to decrease with interaction parameter as $\sqrt{N}$ for $N \geq 6$ (Figure 8). These results agree with the experimental results of Josserand *et al.* (1993). From the plots of angular evolution of surface pressure, the increase of front pressure around the front stagnation point is in line with the hypothesis of Maxworthy (1968, 1969) and Josserand *et al.* (1993) that a stagnant flow develops upstream of the sphere when the magnetic field is increased.

The surface pressure in the upstream zone is approaching an asymptotic value at higher magnetic fields ($N \geq 10$). Such observation is also experimentally reported (Maxworthy, 1968). The isocontours of pressure fields around the cylinder for $Re = 100$, 300 and 500 are shown in Figures 9-11, respectively. From these figures it is evident that with increase of magnetic field the pressure is diminished, recovered and again started diminishing in the downstream zone. These pressure changes are responsible for the non-monotonic behavior of the recirculation length and separation angle observed. The radial and transverse velocity components at $\theta = 90°$ is given in Figure 12 for $Re = 500$.

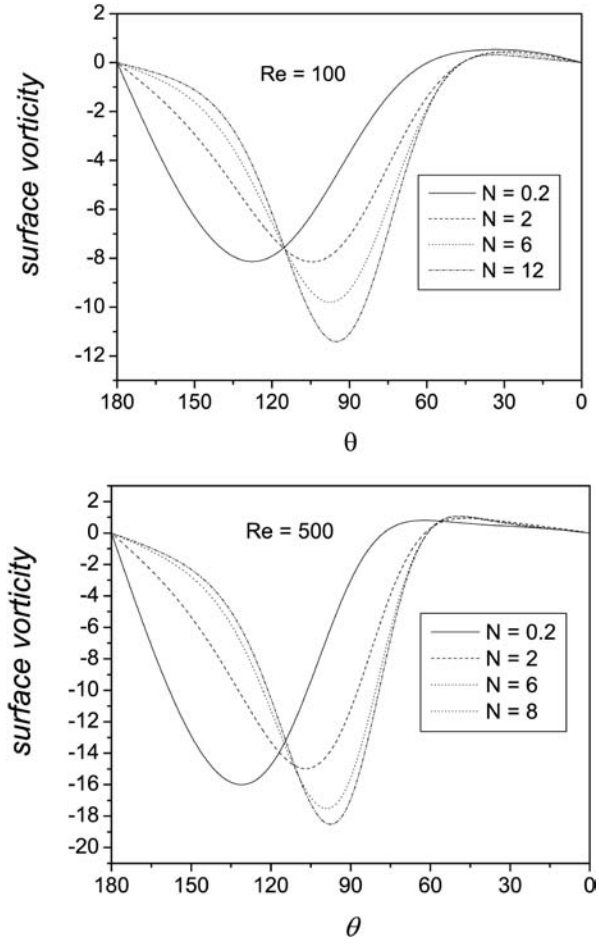

Figure 6.
Angular evolution of surface vorticity for $Re = 100$ and 500

The drag coefficient is calculated using the following relations:

$$\text{Viscous drag coefficient } C_{\mathrm{V}} = -\frac{4\pi}{Re}\int_0^1 \omega_{\xi=0}\sin(\pi\eta)\mathrm{d}\eta \tag{8}$$

$$\text{Pressure drag coefficient } C_P = \frac{4}{Re}\int_0^1 \left(\frac{\partial\omega}{\partial\xi}\right)_{\xi=0}\sin(\pi\eta)\mathrm{d}\eta \tag{9}$$

$$\text{Total drag coefficient } C_{\mathrm{D}} = C_{\mathrm{V}} + C_{\mathrm{P}} \tag{10}$$

The numerical values of the total drag coefficients obtained in 1,024 × 1,024 grid for different values of N are tabulated in Table I. The values obtained in 512 × 512 grid

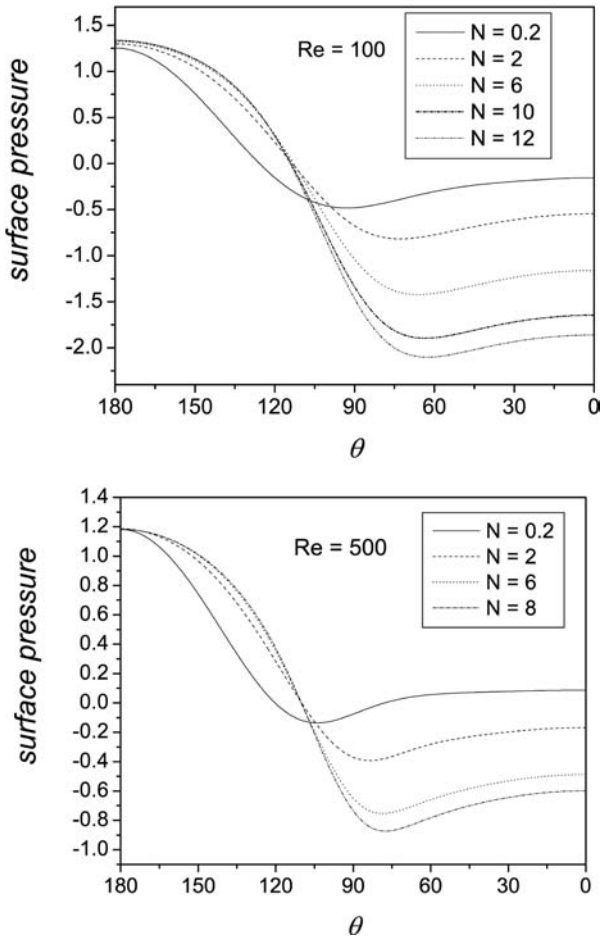

Figure 7.
Angular evolution of surface pressure for $Re = 100$, and 500

are also presented to show grid independence. The pressure drag coefficient C_P and viscous drag coefficient C_V as a function of interaction parameter is shown in Figure 13. From this figure, it can be observed that the pressure drag coefficient increases more rapidly than viscous drag coefficient. The total drag coefficient increases continuously with increase of magnetic field as shown in Figure 14. The constant decrease of the base pressure for high N is the major source of the increase in the overall drag coefficient C_D. For these values of N, the loss in total pressure suffered along the front streamlines under the effect of the $j \times B$ forces are responsible for the rear pressure drop. The pressure drag coefficient C_P and the total drag coefficient C_D are found to increase with interaction parameter as $\sqrt{N}$ when $N \geq 6$. This behavior can be seen in Figure 8. The linear dependence with $\sqrt{N}$ of the pressure drag coefficient and total drag coefficient is in accordance with the experimental findings (Maxworthy, 1968; Yonas, 1967; Josserand *et al.*, 1993).

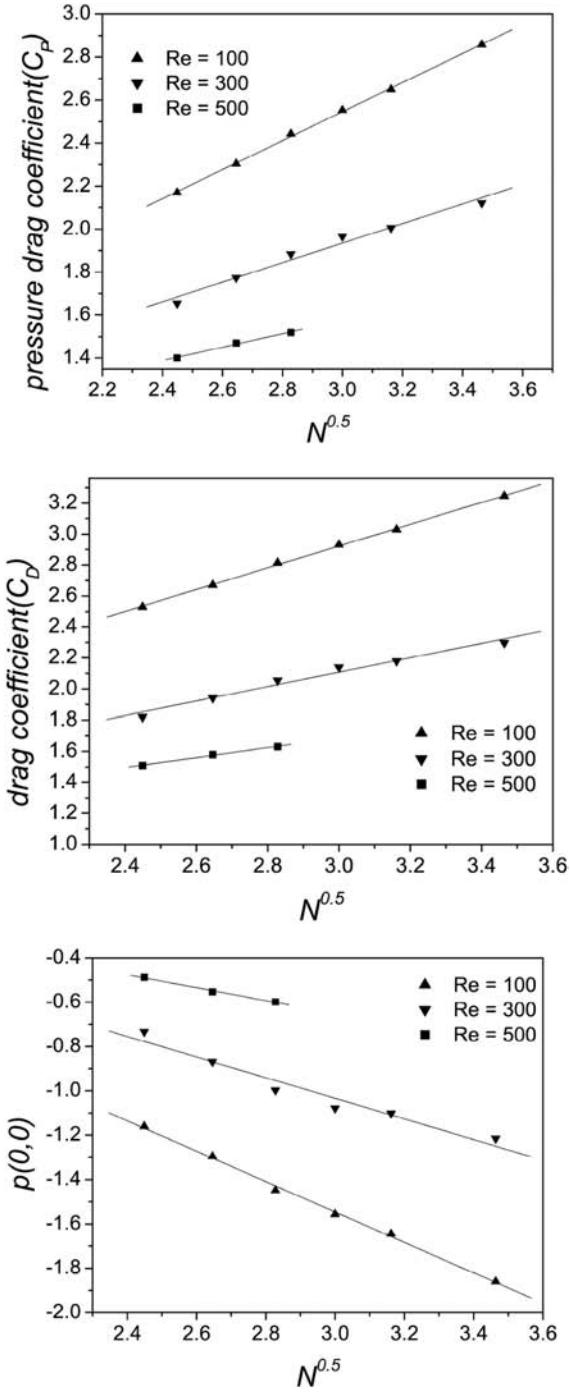

Figure 8.
Linear dependance of pressure drag coefficient C_P, total drag coefficient C_D and the rear pressure $p(0,0)$ on $\sqrt{N}$

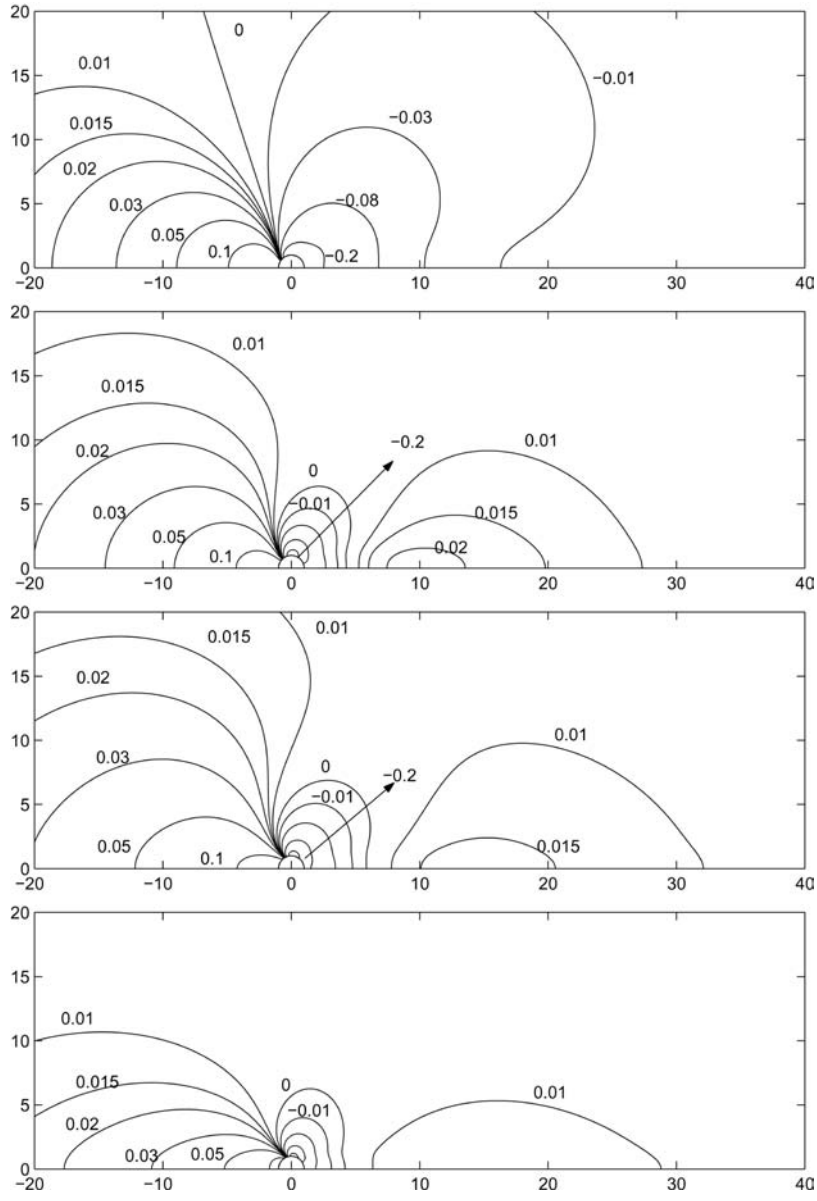

Figure 9.
Pressure fields for the flow with $Re = 100$ and $N = 0.2$, 2, 6 and 12 (top to bottom)

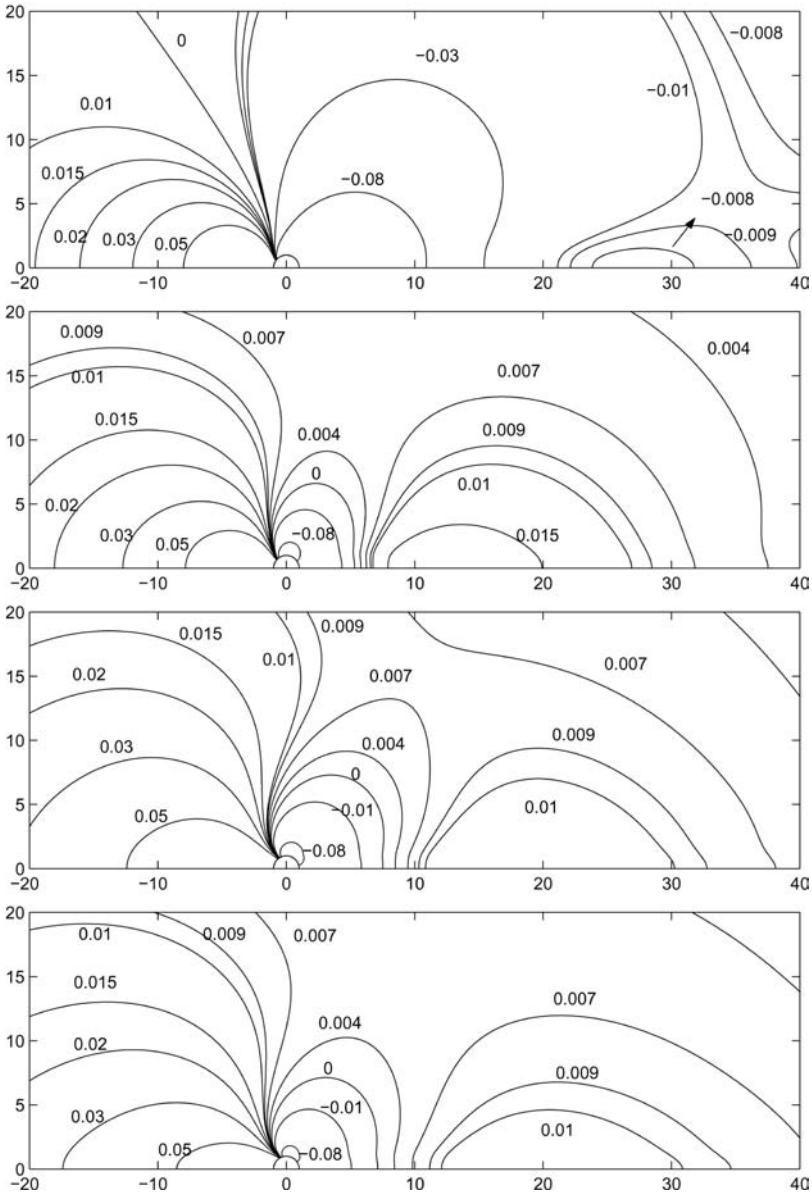

Figure 10.
Pressure fields for the flow with $Re = 300$ and $N = 0.2$, 2, 6 and 12 (top to bottom)

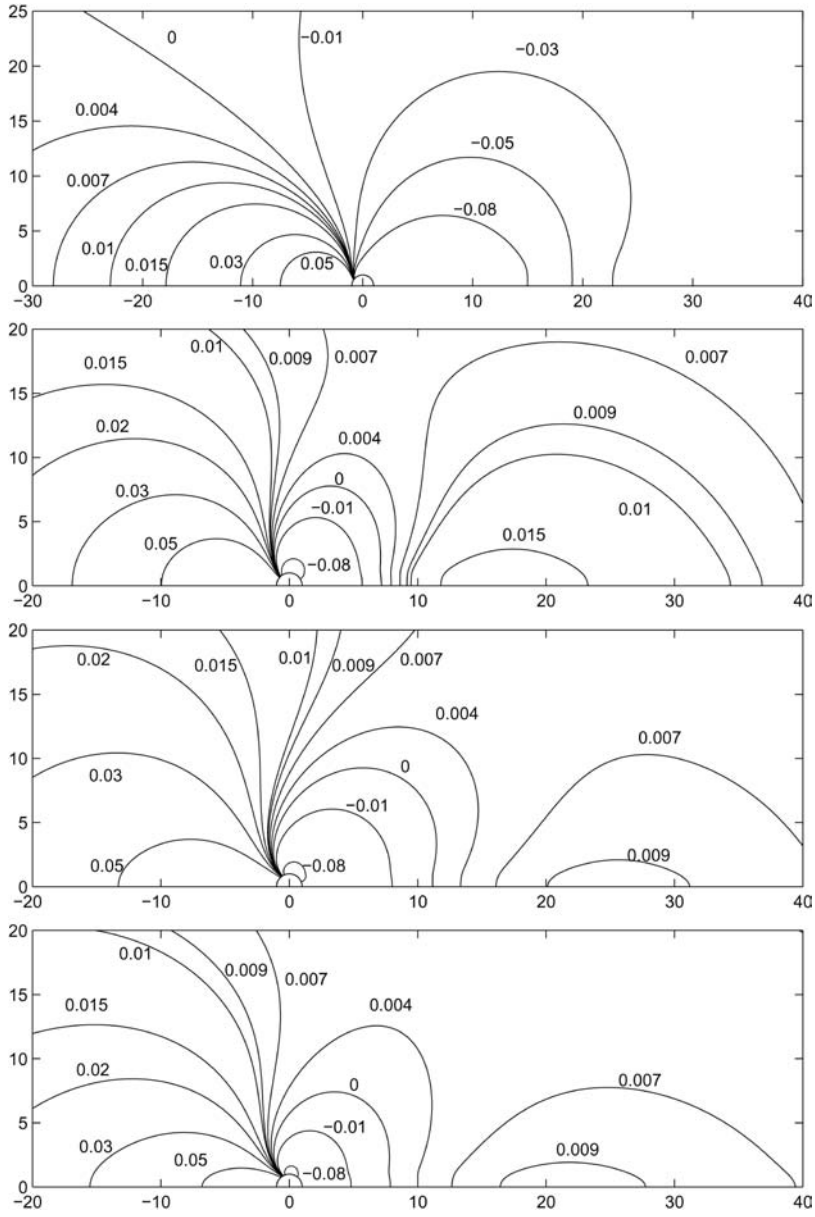

Figure 11.
Pressure fields for the flow with $Re = 500$ and $N = 0.2$, 2, 6 and 8 (top to bottom)

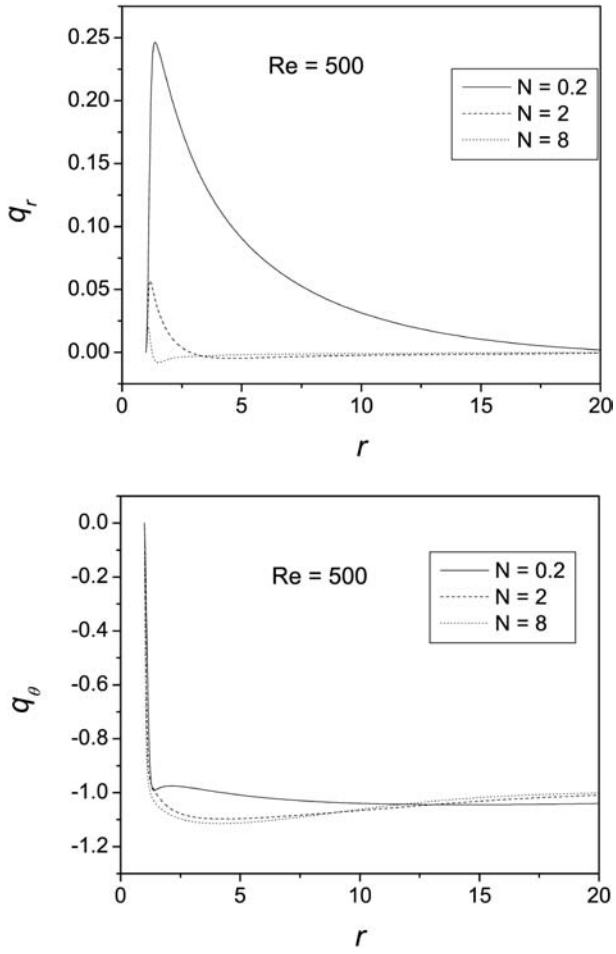

Figure 12.
Variation of radial u and transverse v components of velocity as a function of radial distance, r (far-field distance) for the flow with $Re = 500$ at $\theta = 90°$

	$Re = 100$		$Re = 300$		$Re = 500$	
N	512 × 512	1,024 × 1,024	512 × 512	1,024 × 1,024	512 × 512	1,024 × 1,024
1	1.515	1.517	1.134	1.142	0.958	0.969
2	1.824	1.825	1.367	1.373	1.126	1.135
3	–	2.035	1.509	1.514	1.244	1.253
4	–	2.207	1.624	1.626	1.332	1.340
5	–	2.368	1.722	1.726	–	1.441
6	–	2.530	1.816	1.821	–	1.510
7	–	2.670	–	1.942	–	1.580
8	–	2.814	–	2.056	–	1.631
9	–	2.930	–	2.140	–	–
10	–	3.030	–	2.180	–	–
12	–	3.246	–	2.298	–	–

Table I.
Drag coefficient, C_D values in 512 × 512 and 1,024 × 1,024 grids

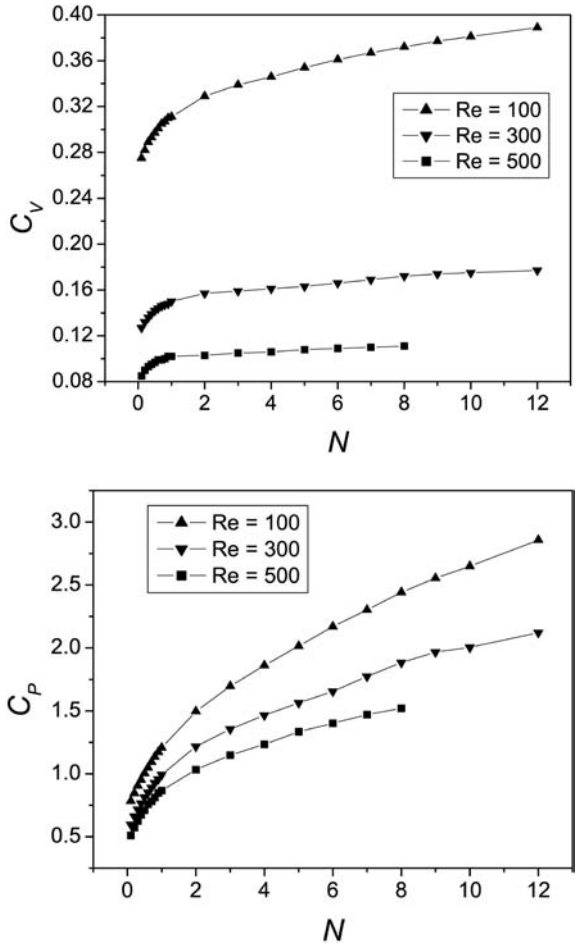

Figure 13.
Variation of viscous drag coefficient C_V and pressure drag coefficient C_P as a function of interaction parameter N

5. Conclusions

The effect of the aligned magnetic field on the steady viscous incompressible and slightly conducting fluid past a circular cylinder is studied at high *Re*s using finite difference method. The pressure Poisson equation is solved to find pressure fields in the flow region. The drag coefficient is found to increase with increase of N. The pressure drag coefficient, total drag coefficient and rear pressure are found to exhibit a linear dependance with $\sqrt{N}$. A non-monotonic behavior in separation angle and separation length is found with the increase of external magnetic field, which is explained using pressure fields. The upstream base pressure is found to increase with increase of N while the downstream base pressure decreases with increase of N.

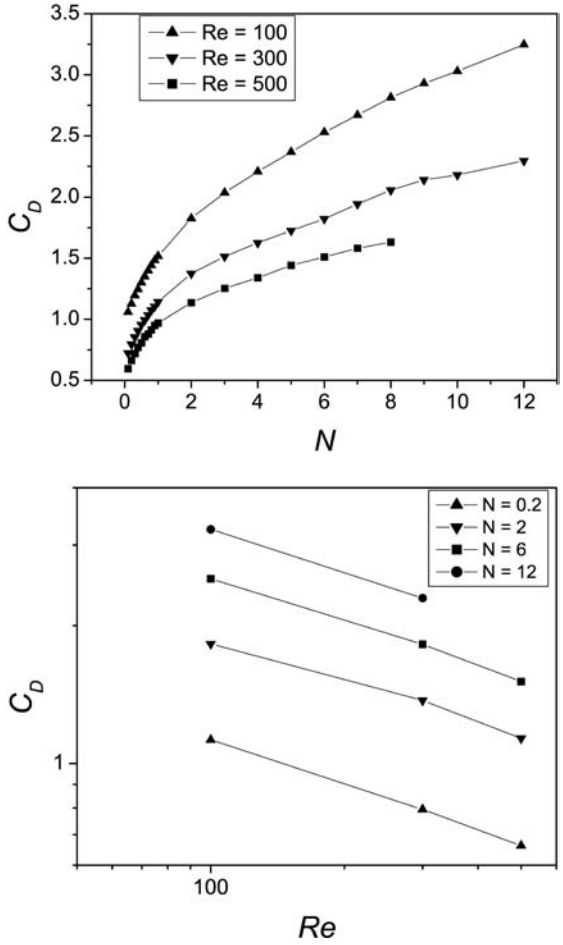

Figure 14.
Variation of total drag coefficient C_D as a function of interaction parameter N (top) and Re (bottom)

References

Bae, H.M., Baranyi, L., Koide, M., Takahashi, T. and Shirakashi, M. (2001), "Suppression of Kármán vortex excitation of a circular cylinder by a second cylinder set downstream in cruciform arrangement", *J. Comp. Appl. Mech.*, Vol. 2, pp. 175-88.

Banks, W.H.H. and Zaturska, M.B. (1984), "The flow of a electrically conducting fluid at a rear stagnation point", *Z für Ang. Math. Physik*, Vol. 35, pp. 72-80.

Baranyi, L. (2003), "Computation of unsteady momentum and heat transfer from a fixed cylinder in laminar flow", *J. Comp. Appl. Mech.*, Vol. 4, pp. 13-25.

Braza, M., Chassaing, P. and Minh, H.H. (1986), "Numerical study and physical analysis of the pressure and velocity fields in the near wake of a circular cylinder", *J. Fluid Mech.*, Vol. 165, pp. 79-130.

Dennis, S.C.R. and Chang, G.Z. (1970), "Numerical solutions for steady flow past a circular cylinder at Reynolds numbers up to 100", *J. Fluid Mech.*, Vol. 42, pp. 471-89.

Fornberg, B. (1980), "A numerical study of steady viscous flow past a circular cylinder", *J. Fluid Mech.*, Vol. 98, pp. 819-55.

Fornberg, B. (1985), "Steady viscous flow past a circular cylinder upto Reynolds numbers 600", *J. Comp. Phys.*, Vol. 61, pp. 297-320.

Fornberg, B. (1988), "Steady viscous flow past a sphere at high Reynolds numbers", *J. Fluid. Mech.*, Vol. 190, pp. 471-89.

Greenblatt, D. and Wyganski, I.J. (2000), "The control of flow separation by periodic excitation", *Prog. Aero. Sci.*, Vol. 36, pp. 487-545.

Henderson, R.D. and Barkely, D. (1996), "Secondary instability in the wake of a circular cylinder", *Phys. Fluids*, Vol. 8, pp. 1683-5.

Jackson, C.P. (1987), "A finite-element study of the onset of vortex shedding in flow past variously shaped bodies", *J. Fluid Mech.*, Vol. 182, pp. 23-45.

Josserand, J., Marty, Ph. and Alemany, A. (1993), "Pressure and drag measurements on a cylinder in a liquid metal flow with an aligned magnetic field", *Fluid Dynamic Research*, Vol. 11, pp. 107-17.

Juncu, G.H. (1999), "A numerical study of steady viscous flow past a fluid sphere", *Int. J. Heat and Fluid Flow*, Vol. 20, pp. 414-21.

Kawamura, T. and Kuwahara, K. (1984), "Computation of high Reynolds number flow around a circular cylinder with surface roughness", *Proceedings of the 22nd Aerospace Sciences Meeting, Reno, Nevada*, AIAA-84-0340, pp. 1-11.

Lahjomri, J., Caperan, P. and Alemany, A. (1993), "The cylinder wake in a magnetic field aligned with the velocity", *J. Fluid Mech.*, Vol. 253, pp. 421-48.

Leibovich, S. (1967), "Magnetohydrodynamic flow at a rear stagnation point", *J. Fluid Mech.*, Vol. 29, pp. 401-13.

Lima E Silva, A.L.F., Silveira-Neto, A. and Damasceno, J.J.R. (2003), "Numerical simulation of two-dimensional flows over a circular cylinder using the immersed boundary method", *J Comp. Phys.*, Vol. 189, pp. 351-70.

Maxworthy, T. (1968), "Experimental studies in magneto-fluid dynamics: pressure distribution measurements around a sphere", *J. Fluid Mech.*, Vol. 31, pp. 801-14.

Maxworthy, T. (1969), "Experimental studies in magneto-fluid dynamics: flow over a sphere with a cylindrical afterbody", *J. Fluid Mech.*, Vol. 35, pp. 411-6.

Mutschke, G., Gerbeth, G. and Shatrov, V. (1997), "Two- and three-dimensional instabilities of the cylinder wake in an aligned magnetic field", *Phys. Fluids*, Vol. 9, pp. 3114-6.

Mutschke, G., Gerbeth, G., Shatrov, V. and Tomboulides, A. (2001), "The scenario of three-dimensional instabilities of the cylinder wake in an external magnetic field: a linear stability analysis", *Phys. Fluids*, Vol. 13, pp. 723-34.

Mutschke, G., Shatrov, V. and Gerbeth, G. (1998), "Cylinder wake control by magnetic fields in liquid metal flows", *Expt. Thermal and Fluid Sci.*, Vol. 16, pp. 92-9.

Norberg, C. (2003), "Fluctuating lift on a circular cylinder: review and new measurements", *J. Fluids and Structures*, Vol. 17, pp. 57-96.

Raghava Rao, C.V. and Sekhar, T.V.S. (1993), "Numerical solution of the slow translation of a sphere moving along the axis of a rotating viscous fluid", *Comp. Fluid Dyn.*, Vol. 1, pp. 351-9.

Raghava Rao, C.V. and Sekhar, T.V.S. (1995), "Translation of a sphere in a rotating viscous fluid – a numerical study", *Int. J. Numer. Methods in Fluids*, Vol. 20, pp. 1253-62.

Robert Leigh Underwood (1969), "Calculation of incompressible flow past a circular cylinder at moderate Reynolds number", *J. Fluid Mech.*, Vol. 37, pp. 95-114.

Sekhar, T.V.S., Sivakumar, R. and Ravi Kumar, T.V.R. (2005), "Magnetohydrodynamic flow around a sphere", *Fluid Dynamics Research*, Vol. 37, pp. 357-73.

Takami, H. and Keller, H.B. (1969), "Steady two-dimensional viscous flow of an incompressible fluid past a circular cylinder", *Phys. Fluids*, Vol. II, pp. 51-6.

Tang, T. and Ingham, D.B. (1991), "On steady flow past a rotating circular cylinder at Reynolds numbers 60 and 100", *Computers & Fluids.*, Vol. 19, pp. 217-30.

Thompson, M.C. and Le Gal, P. (2004), "The Stuart-Landau model applied to wake transition revisited", *European J. Mech B/Fluids*, Vol. 23, pp. 219-28.

Weir, T., Fey, U., Gerbeth, G., Mutschke, G. and Avilov, V. (2000), "Boundary layer control by means of electromagnetic forces", *Eur. Res. Community on Flow, Turbulence and Combustion (ERCOFTAC) Bull.*, Vol. 44, pp. 36-40.

Weir, T., Fey, U., Gerbeth, G., Mutschke, G., Lielausis, O. and Platacis, E. (2001), "Boundary layer control by means of wall parallel Lorentz forces", *Magnetohydrodynamics*, Vol. 37 Nos 1/2, pp. 177-86.

Weir, T., Gerbeth, G., Mutschke, G., Lielausis, O. and Lammers, G. (2003), "Control of flow separation using electromagnetic forces", *Flow, Turbulence and Combustion*, Vol. 71, pp. 5-17.

Weir, T., Gerbeth, G., Mutschke, G., Platacis, E. and Lielausis, O. (1998), "Experiments on cylinder wake stabilization in an electrolyte solution by means of electromagnetic forces localized on the cylinder surface", *Exp. Thermal Fluid Sci.*, Vol. 16, pp. 84-91.

Welliamson, C.H.K. (1989), "Oblique and parallel modes of vortex shedding in the wake of a circular cylinder at low Reynolds number", *J. Fluid Mech.*, Vol. 206, pp. 579-627.

Wesseling, P. (1980), *Report NA-37*, Delft University of Technology, The Netherlands.

Williamson, C.H.K. (1996a), "Vortex dynamics in the cylinder wake", *Ann. Rev. Fluid Mech.*, Vol. 28, pp. 477-539.

Williamson, C.H.K. (1996b), "Model a secondary instability in wake transition", *Phys. Fluids*, Vol. 8, pp. 1680-2.

Yonas, G. (1967), "Measurements of drag in a conducting fluid with an aligned magnetic field and large interaction parameter", *J. Fluid Mech.*, Vol. 30, pp. 813-21.

Corresponding author
T.V.S. Sekhar can be contacted at: sekhartvs@yahoo.co.in